

# Suzaku and Chandra Observations of CIZA J1700.8–3144, a Cluster of Galaxies in the Zone of Avoidance

Hideyuki MORI,<sup>1,2</sup> Yoshitomo MAEDA,<sup>3</sup> Yoshihiro UEDA,<sup>4</sup> Kazuhiro NAKAZAWA,<sup>5</sup> Yuzuru TAWARA,<sup>6</sup>

<sup>1</sup>CRESST and X-ray Astrophysics Laboratory, NASA Goddard Space Flight Center, Greenbelt, MD 20771, USA

<sup>2</sup>Department of Physics, University of Maryland, Baltimore County, 1000 Hilltop Circle, Baltimore, MD 21250, USA

<sup>3</sup>Department of Space Astronomy and Astrophysics, Institute of Space and Astronautical Science (ISAS), Japan Aerospace Exploration Agency (JAXA), 3-1-1, Yoshinodai, Chuo-ku, Sagami-hara, 252-5210

<sup>4</sup>Department of Astronomy, Graduate School of Science, Kyoto University, Sakyo-ku, Kyoto, 606-8502

<sup>5</sup>Department of Physics, School of Science, The University of Tokyo, 7-3-1, Hongo, Bunkyo-ku, Tokyo, 113-0033

<sup>6</sup>Division of Particle and Astrophysical Science, Graduate School of Science, Nagoya University, Furo-cho, Chikusa-ku, Nagoya, 464-8602

\*E-mail: hideyuki.mori@nasa.gov

Received (reception date); Accepted (acceptation date)

## Abstract

We present the Chandra and Suzaku observations of 1RXS J170047.8–314442, located towards the Galactic bulge, to reveal a wide-band (0.3–10 keV) X-ray morphology and spectrum of this source. With the Chandra observation, no point source was found at the position of 1RXS J170047.8–314442. Alternatively, we revealed the presence of diffuse X-ray emission by the wide-band X-ray image obtained from the Suzaku XIS. Although the X-ray emission had a nearly circular shape with a spatial extent of  $\sim 3'.5$ , the surface brightness profile was not axisymmetric; a bright spot-like emission was found at  $\sim 1'$  away in the north-western direction from the center. The radial profile of the surface brightness, except for this spot-like emission, was reproduced with a single  $\beta$ -model;  $\beta$  and the core radius were found to be 1.02 and  $1'.51$ , respectively. The X-ray spectrum of the diffuse emission showed an emission line at  $\sim 6$  keV, indicating an origin of a thermal plasma. The spectrum was well explained with an absorbed optically-thin thermal plasma model with a temperature of 6.2 keV and a redshift parameter of  $z = 0.14 \pm 0.01$ . Hence, the X-ray emission was considered to arise from the hot gas associated with a cluster of galaxies. Our spectroscopic result confirmed the optical identification of 1RXS J170047.8–314442 by Kocevski et al. (2007): CIZA J1700.8–3144, a member of the cluster catalogue in the Zone of Avoidance. The estimated bolometric X-ray luminosity of  $5.9 \times 10^{44}$  erg s<sup>−1</sup> was among the lowest with this temperature, suggesting that this cluster is far from relaxed.

**Key words:** X-rays: galaxies: clusters<sub>1</sub> — X-rays: individual (1RXS J170047.8–314442)<sub>2</sub> — X-rays:

individual (CIZA J1700.8–3144)<sub>3</sub>

## 1 Introduction

Population studies of the Galactic components are a key issue to understand the dynamical formation of the Galaxy. X-ray sources containing compact objects, such as neutron stars and black holes, are useful as a tracer of the primordial high-mass ( $M > 8M_{\odot}$ ) population. Thus, focusing on the Galactic bulge (Carollo et al. 1999), we first constructed a flux-limited ( $\gtrsim 10^{-12}$  erg s $^{-1}$  cm $^{-2}$ ) sample of the X-ray sources towards this region (Mori et al. 2006) extracted from the ROSAT All-Sky Survey Bright Source Catalogue (RBSC; Voges et al. 1999). However, about half ( $\sim 40$ ) of this bulge sample has been still unidentified. To improve the completeness of the sample, our team has been working on the identification of the Galactic bulge sources with X-ray spectroscopic observations above 2 keV (e.g., Mori et al. 2012).

In this on-going project, we found that one of the unidentified sources was a cluster of galaxies at  $z = 0.13$  (Mori et al. 2013). Our result implies that clusters of galaxies may occupy a non-negligible fraction of the bright X-ray sources towards the Galactic bulge. Because of low Galactic latitudes, moderate X-ray absorption as well as severe optical extinction hampers detailed spectroscopic studies of the clusters in the bulge region.

In this paper, we report the results of the Suzaku and Chandra observations of 1RXS J170047.8–314442. This source was unidentified when we started our project to clarify the X-ray source population in the Galactic bulge. Later, Kocevski et al. (2007) identified it with CIZA J1700.8–3144, a cluster of galaxies in the CIZA catalogue. The authors picked up cluster candidates from the RBSC, and then carried out the *R*-band optical imaging survey to detect their member galaxies. From the spectroscopic observation to three member galaxies, Kocevski et al. (2007) also reported the redshift parameter ( $z = 0.134$ ) of CIZA J1700.8–3144. Because of the limited sensitivity of the ROSAT PSPC (0.1–2.4 keV), however, spatial and spectral information on X-ray emission above 2 keV associated with this cluster of galaxies is still unclear.

The paper is organized as follows. Brief information on the observations and the data used in the analysis is mentioned in section 2. We describe the image and spectral analysis in section 3. The X-ray properties of the observed diffuse emission are discussed in section 4. Then, a summary of the observations is given in section 5. Throughout the paper, the cosmological parameters are assumed to be  $H_0 = 70$  km s $^{-1}$  Mpc $^{-1}$  (Hubble constant),  $\Omega_M = 0.27$  (density parameter of matter), and  $\Omega_{\Lambda} = 0.73$  (density parameter of dark energy). Errors represent the 90% confidence limits unless otherwise stated.

## 2 Observation and data reduction

We observed 1RXS J170047.8–314442 with Chandra (Weisskopf et al. 2000) on April 20, 2012. To handle the expected source flux, here we operated only the S3 chip of the Advanced CCD Imaging Spectrometer (ACIS; Burke et al. 1997) in the very faint format. The 128-pixel subarray model was also applied to avoid the pile-up effect. No grating module was employed. The log of the Chandra observation is given in table 1. The level 2 event files generated with the standard data processing were used in the following analysis. Scientific products were created with the Chandra Interactive Analysis of Observations (CIAO, version 4.5; Fruscione et al. 2006)<sup>1</sup>.

The 1RXS J170047.8–314442 observation with Suzaku (Mitsuda et al. 2007) was performed to obtain the X-ray spectrum above 2 keV on February 18, 2013. We show the observation log in table 1. Suzaku enables us to carry out imaging spectroscopy in the 0.2–10 keV band with the combination of the X-ray CCD cameras (XIS; Koyama et al. 2007) and the X-ray Telescopes (XRT; Serlemitsos et al. 2007). Owing to the XIS2 failure, two front-illuminated (FI) CCDs (XIS0 and XIS3) and one back-illuminated (BI) CCD (XIS1) were available. The XIS was operated with the normal clocking mode without any window and burst options. The Spaced-row Charge Injection (SCI; Uchiyama et al. 2009) was applied to mitigate the charge transfer inefficiency. Suzaku also possesses a non-imaging hard X-ray detector (HXD; Takahashi et al. 2007, Kokubun et al. 2007) that consists of PIN Si diodes and well-type GSO/BGO scintillators to cover an energy range of 10–600 keV.

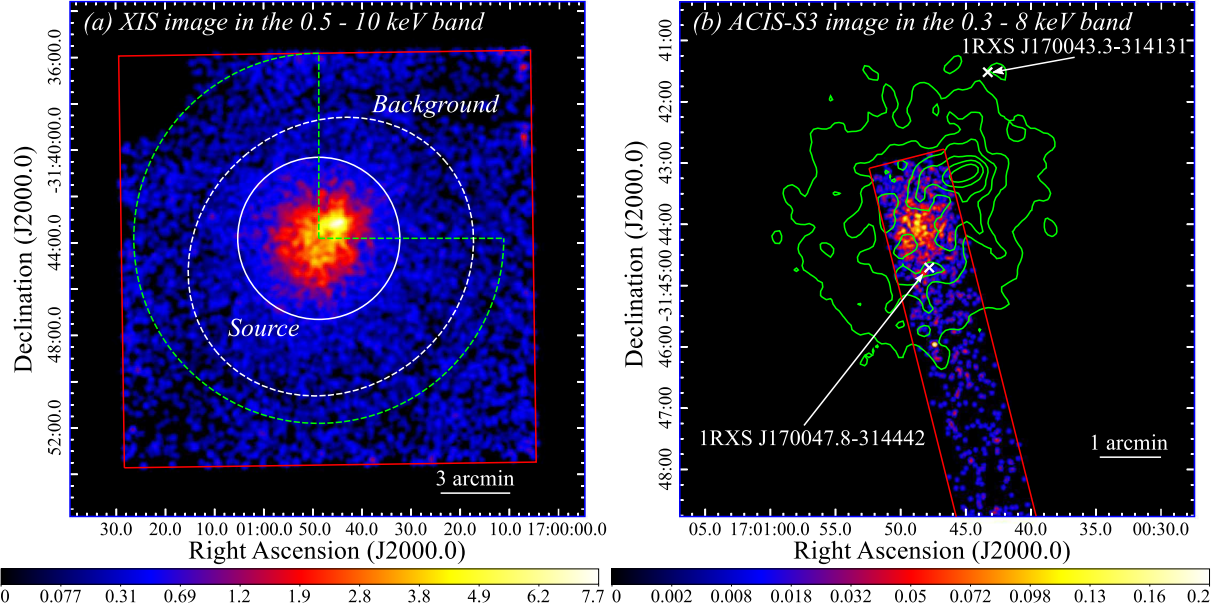
We analyzed cleaned event data that had already been pre-processed with the Suzaku team; the processing version is 2.8.20.35. While the exposure time of the XIS was 8.9 ks, the dead-time corrected one of the HXD was 7.7 ks. We used the HEASOFT version 6.15 and the latest calibration database to create scientific products. We note that the HXD count rate in the 18–40 keV band was  $0.160 \pm 0.005$  cts s $^{-1}$ . The count rate of Non X-ray Background (NXB) was derived to be  $0.153 \pm 0.001$  cts s $^{-1}$  from `ae407027010_hxd_pinbgd.evt`, the “tuned” background file provided from the HXD team. Since the contribution of the Cosmic X-ray Background (CXB) was estimated to be 0.01 cts s $^{-1}$ , no significant signal was detected from the HXD. Therefore, we focus on the XIS data in the following analysis.

<sup>1</sup> <http://cxc.harvard.edu/ciao/>

**Table 1.** Observation log.

	Obs. ID	Start time (UT)	End time (UT)	Exposure* (ks)
Chandra	12939 <sup>†</sup>	2012/04/20 05:06:32	2012/04/20 06:35:26	3.69 (ACIS-S3)
Suzaku	407027010	2013/02/18 11:50:13	2013/02/18 18:00:11	8.93 (XIS), 7.65 (HXD)

\* Effective exposure of the screened data. The HXD exposure is dead-time corrected.

<sup>†</sup> Sequence number is 900971.

**Fig. 1.** (a) XIS image of 1RXS J170047.8–314442 in the 0.5–10 keV band. A  $4''.1 \times 4''.1$  binning, the smoothing with a Gaussian function of  $\sigma = 12''.5$ , and the vignetting correction were applied to the XIS image. The source and background-extraction regions are indicated with a white solid circle and its surrounding dashed ellipse, respectively. The radial profile of the X-ray surface brightness (see figure 3) was obtained from the green dashed sector. (b) ACIS-S3 image in the 0.3–8 keV band. The image was smoothed with a Gaussian function of  $\sigma = 3''$ . The positions of 1RXS J170047.8–314442 and 1RXS J170043.3–314131, another unidentified X-ray source, listed in the RBSC are represented with white crosses. Green contours show the surface brightness of the XIS image. The contour levels are linearly spaced from 6.6 to 1.1 cts per  $4''.1 \times 4''.1$ . Red squares in both panels represent the field of views of the (a) XIS and (b) ACIS-S3 operated with the 128-pixel subarray mode. The color scales at the bottom are in unit of (a) photons per  $4''.1 \times 4''.1$  and (b) photons per  $0''.5 \times 0''.5$ .

### 3 Analysis

#### 3.1 X-ray image

The vignetting-corrected XIS image of 1RXS J170047.8–314442 in the 0.5–10 keV band is shown in figure 1a. We found diffuse X-ray emission at the center of the XIS field of view, positionally coincident with 1RXS J170047.8–314442. Thus, we consider this diffuse emission as 1RXS J170047.8–314442 hereafter. Although the emission had a nearly circular shape, its surface brightness profile was not axisymmetric. The position of the peak brightness was  $(RA, Dec)_{J2000.0} = (17^h00^m44^s.9, -31^\circ43'09'')$ , located  $\sim 1'$  away in the north-western direction from the center of the X-ray emission.

We also show the ACIS-S3 image in the 0.3–8 keV band in figure 1b. No point source was found at the position of 1RXS J170047.8–314442 (white cross in figure 1b). Alternatively, we detected extended emission similar to that in the XIS image. The brightness peak was unfortunately located outside of the

ACIS-S3 field of view. However, the surface brightness around the peak was not so high in the ACIS-S3 image. Therefore, the size of the north-western spot-like emission was estimated to be at most  $30''$ .

Coming back to the XIS data, we indicate regions to extract the source and background spectra with a white solid circle and a white dashed ellipse, respectively, in figure 1a. We selected the source-extraction region with a radius of  $3''.5$  so that the surface brightness at the boundary reduces to  $\sim 5\%$  of the peak brightness. The center of the circle was chosen to be  $(RA, Dec)_{J2000.0} = (17^h00^m48^s.8, -31^\circ43'49'')$ . The major and minor axes of the surrounding background region were set to be parallel to the Galactic latitude and longitude, respectively, by taking into consideration the spatial distribution of the Galactic Ridge X-ray Emission (GRXE; Koyama et al. 1986). The outer radii of the background region were  $6''.43$  (major axis) and  $5''.73$  (minor axis). The redistribution matrix file (RMF) and ancillary response file (ARF) were created with `xismfgen` and `xissimarfgen` (Ishisaki et al. 2007), respectively. We note that

the background-subtracted count rates in the 0.5–10 keV band were  $0.26 \pm 0.01$  (XIS0),  $0.30 \pm 0.01$  (XIS1), and  $0.24 \pm 0.01$  (XIS3)  $\text{cts s}^{-1}$ . Since the light curves did not exhibit any significant variability, we analyzed the summed data during the whole observation.

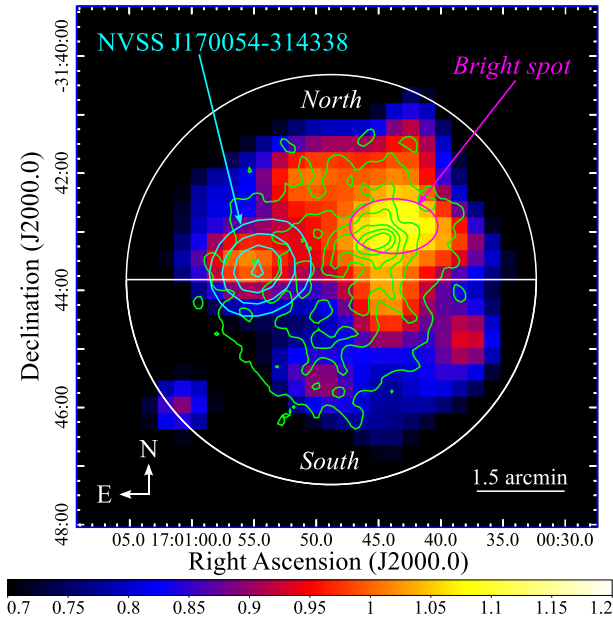


**Fig. 2.** Color map of the hardness ratio defined as  $H/L$ , where  $H$  and  $L$  represent X-ray photons within  $17'' \times 17''$  in the 2–10 keV and 0.5–2 keV bands, respectively. Green contours are the same as those shown in figure 1b. A magenta ellipse indicates the region to extract the “Bright spot” spectra. The definition of the “South” and “North” regions is described in the text. Cyan contours display the intensity at 1.4 GHz from 8 mJy to 2 mJy obtained from the NRAO VLA Sky Survey (NVSS). In the NVSS catalogue, this radio source is listed as NVSS J170054–314348.

To examine spectral properties under poor photon statistics, we further made a color map of a hardness ratio (HR) given as  $H/L$ , where  $H$  and  $L$  represent the photon counts in the 2–10 keV and 0.5–2 keV bands, respectively. The NXB-subtracted images in the soft and hard X-ray bands were binned with  $17'' \times 17''$ . The HR map is shown in figure 2. The HRs in the X-ray bright north-western region of 1RXS J170047.8–314442 tend to be higher than those of the south-eastern and outskirt regions. Thus, we divided the source-extraction region into three regions, designated as “Bright spot”, “North”, and “South”, for the following spectral analysis. Meanwhile, the source-extraction region was defined explicitly to be “whole source” region hereafter. The “Bright spot” region was selected so that the HR was larger than 1.05. This region was an ellipse centered on  $(RA, Dec)_{J2000.0} = (17^{\text{h}}00^{\text{m}}43^{\text{s}}.8, -31^{\circ}42'54'')$ . The radii of the major and minor axes of the “Bright spot” region were  $45''$  and  $28''$ , respectively. While the “South” region was defined as the southern semicircle of the source-extraction region, the “North” region was set to be the northern one excluding the “Bright spot” region.

In order to calculate the ARF accurately, we need a 2-dimensional distribution of the X-ray intensity of 1RXS J170047.8–314442. Since the observed X-ray emission was not axisymmetric, we first made a radial profile of the surface brightness from a sector shown in figure 1a, where the north-western bright spot was removed. The resultant radial profile is shown in figure 3. We fitted the profile with a single  $\beta$ -model (Cavaliere & Fusco-Femiano 1976), taking into account the point spread function (PSF) of the XRT and the contribution from the underlying diffuse emission: NXB, GRXE, and CXB. The fitting prescription we used here was the same as that described in Mori et al. (2013). The combined model of  $(\beta, r_c) = (1.02, 1'.51)$  yielded a marginally acceptable fit with  $\chi^2 = 70/48$  d.o.f.. The 68% confidence limits were  $\beta = 1.02^{+0.10}_{-0.08}$  and  $r_c = 1'.51^{+0.16}_{-0.15}$ .

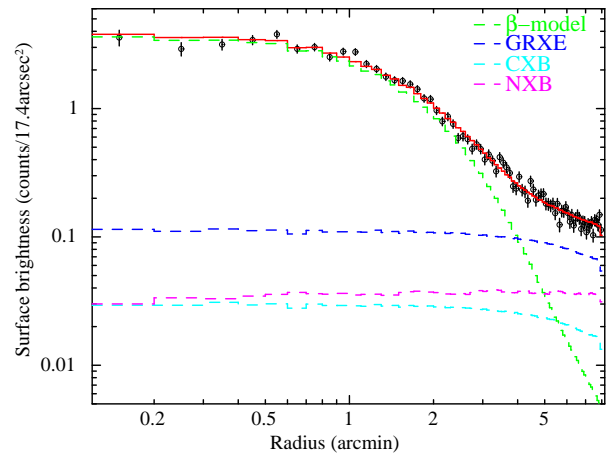


**Fig. 3.** Radial profile of the surface brightness of 1RXS J170047.8–314442 in the 0.5–10 keV band (open circles). A vertical bar on each data point indicates a  $1\sigma$  statistical error. The red solid line represents the best-fit combined model that consists of the  $\beta$ -model with  $(\beta, r_c) = (1.02, 1'.51)$  (green), GRXE (blue), CXB (cyan), and NXB (magenta dashed line) components.

Since the angular resolutions of the Suzaku XRTs are limited to be  $\sim 2'$  (Serlemitsos et al. 2007), the spatial structure of the north-western “Bright spot” region cannot be fully resolved. Thus, for simplicity of the ARF calculation, we modelled this emission as a single point source. After subtracting the simulated images of the GRXE, CXB, NXB, and  $\beta$ -model components from the raw XIS image, we determined the source position to be  $(RA, Dec)_{J2000.0} = (17^{\text{h}}00^{\text{m}}44^{\text{s}}.6, -31^{\circ}43'09'')$ . The normalization of the point source was set so as to reproduce the ratio of the observed X-ray counts between the point source and  $\beta$ -model components. We made hereafter some ARF files using a sky image that consists of the  $\beta$ -model with  $(\beta, r_c) = (1.02, 1'.51)$  and this point source. Hence, X-ray spectra represent a weighted average of the source spectrum over the extraction region we chose.



## 3.2 X-ray spectrum

data and folded model

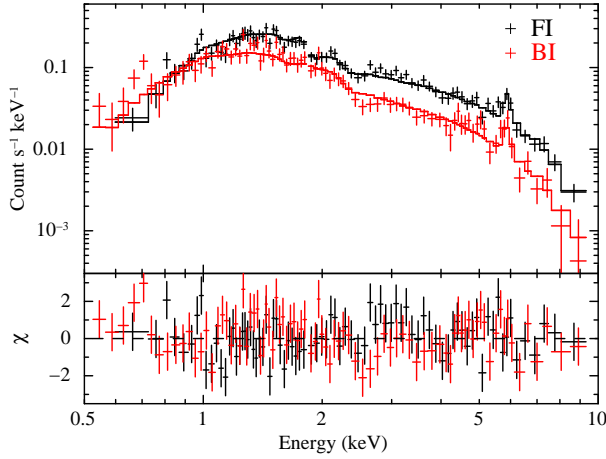


**Fig. 4.** X-ray spectra of 1RXS J170047.8–314442 obtained with the FI (black pluses) and BI (red pluses) CCDs. The best-fit optically-thin thermal plasma model is indicated with the black and red solid lines.

The X-ray spectra of the whole source region obtained with the FI and BI CCDs are shown in figure 4. The XIS0 and XIS3 spectra were averaged to increase the photon statistics. In the spectral fit, we excluded spectral bins around the Si-K edge (1.82–1.84 keV) because of the uncertainty of the quantum efficiency. The presence of the clear emission line at 5.9 keV indicates that the X-ray source is not an object in the Galaxy. In addition, the spatially extended X-ray emission combined with its convex shape suggests that the source has a thermal origin. Then, we fitted the spectra with an optically-thin thermal plasma model in collisional ionization equilibrium (*apec* in XSPEC; Balucinska-Church & McCammon 1992). Here, we adopted the solar abundance given by Anders & Grevesse (1989). We also set the redshift parameter free. The absorbed thin-thermal plasma model gave a good fit with  $\chi^2 = 177/161$  d.o.f. and null hypothesis probability of 19%. The best-fit parameters are summarized in table 2. The absorption column density, plasma temperature, metal abundance, and redshift parameter were  $N_H = (2.4 \pm 0.4) \times 10^{21} \text{ cm}^{-2}$ ,  $kT = 6.2 \pm 0.7 \text{ keV}$ ,  $Z/Z_\odot = 0.26 \pm 0.08$ , and  $z = 0.14 \pm 0.01$ , respectively. The X-ray flux in the 0.5–10 keV band was  $6.0 \times 10^{-12} \text{ erg s}^{-1} \text{ cm}^{-2}$ .

Next, we fitted the “South”, “North”, and “Bright spot” spectra with an absorbed optically-thin thermal plasma model, as is shown in figure 5. The background spectrum for these spectra was the same as that extracted from the background region. While the “Bright spot” spectra were grouped to contain at least 20 photons in each spectral bin, the “South” and “North” spectra were binned with 30 photons for the FI and 25 photons for the BI. For the “South” and “North” spectra, we obtained acceptable fits with  $\chi^2 = 139/137$  d.o.f. (South) and  $\chi^2 = 126/126$  d.o.f. (North). The plasma temperature in the

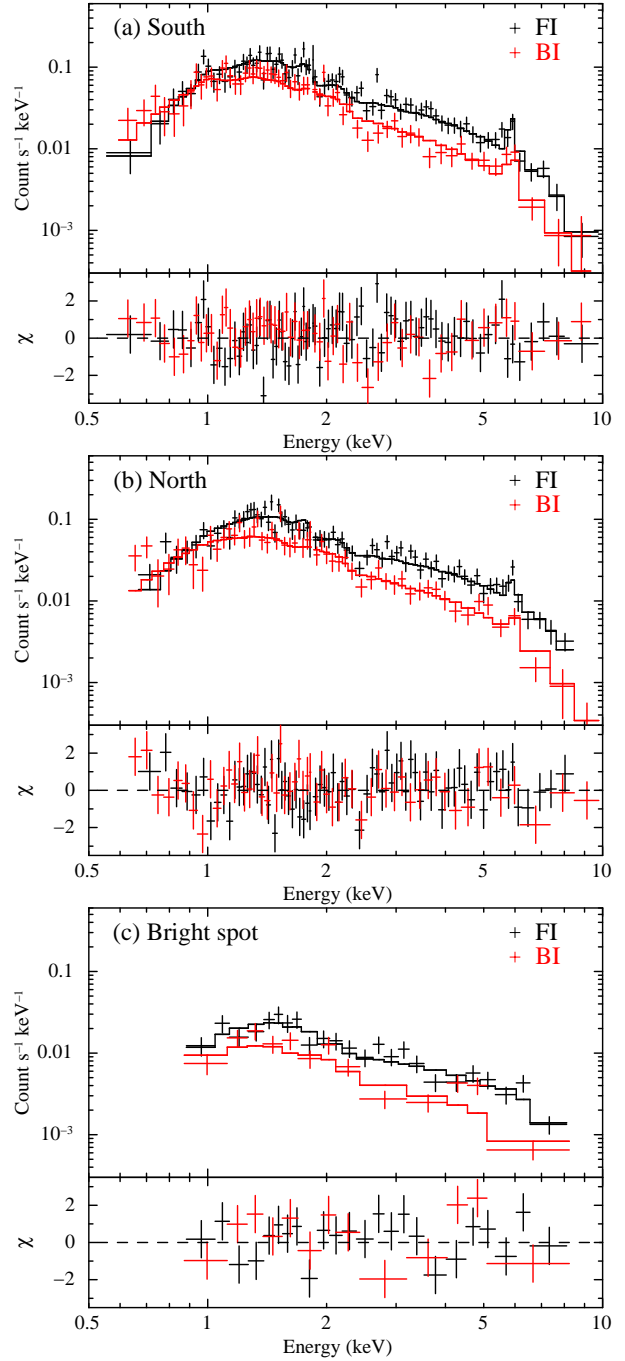


**Fig. 5.** X-ray spectra of 1RXS J170047.8–314442 extracted from the (a) “South”, (b) “North”, and (c) “Bright spot” regions. Marks and colors are the same as those in figure 4.

**Table 2.** Best-fit parameters of the 1RXS J170047.8–314442 spectra\*.

Parameters	Model : apec <sup>†</sup>			
	Whole source	South	North	Bright spot
$N_{\mathrm{H}}$ ( $10^{21} \text{ cm}^{-2}$ )	$2.4 \pm 0.4$	$2.5 \pm 0.6$	$2.4^{+0.7}_{-0.5}$	$2.6^{+1.6}_{-1.2}$
$kT$ (keV)	$6.2 \pm 0.7$	$5.0^{+0.7}_{-0.6}$	$6.9^{+1.6}_{-0.9}$	$10^{+9}_{-4}$
$Z/Z_{\odot}$ <sup>‡</sup>	$0.26 \pm 0.08$	$0.35^{+0.13}_{-0.12}$	$0.24^{+0.14}_{-0.13}$	0.26 (fixed)
Redshift $z$	$0.14 \pm 0.01$	$0.137 \pm 0.008$	$0.14^{+0.03}_{-0.01}$	0.14 (fixed)
$EM$ <sup>§</sup>	$(6.0^{+0.4}_{-0.3}) \times 10^{-3}$	$(6.1^{+0.5}_{-0.6}) \times 10^{-3}$	$(5.6^{+0.5}_{-0.2}) \times 10^{-3}$	$(5.9^{+1.1}_{-0.6}) \times 10^{-3}$
$\chi^2/\text{d.o.f.}$	177/161 = 1.1	139/137 = 1.0	126/126 = 1.0	48/33 = 1.5
Flux <sup>l</sup> ( $10^{-12} \text{ erg s}^{-1} \text{ cm}^{-2}$ )	6.0	5.7	5.9	7.0

\* Superscript and subscript figures represent the upper and lower limits of the 90% confidence interval, respectively.

<sup>†</sup> Model components defined in XSPEC.

<sup>‡</sup> Elemental abundances relative to solar (Anders & Grevesse 1989).

<sup>§</sup> In unit of  $10^{-14} / (4\pi D^2) \int n_e n_H dV \text{ cm}^{-5}$ . Here  $V$  and  $D$  are the volume and distance to the plasma, respectively.

<sup>l</sup> X-ray fluxes in the 0.5–10 keV band.

“South” region was found to be significantly lower than that in the “North” region (see table 2), although its significance was at most  $2.9\sigma$  level.

Since the emission feature at  $\sim 6$  keV was obscure in the “Bright spot” spectra, we fixed the redshift and metal abundance to be 0.14 and 0.26, respectively. Although the model yielded a marginally acceptable fit of  $\chi^2 = 48/33$  d.o.f., the best-fit temperature of  $kT = 10^{+9}_{-4}$  keV was again larger than that in the “South” region ( $kT = 5.0^{+0.7}_{-0.6}$  keV) with  $1.9\sigma$  significance.

Furthermore, we tried to fit the “Bright spot” spectra with several different models. When employing the absorbed thin-thermal plasma model, in which the redshift and metal abundance were set to be free, the  $\chi^2$  value decreased to be 43 (31 d.o.f.). The best-fit parameters did not change, except for the redshift parameter:  $z = 0.41^{+0.07}_{-0.08}$ . This larger redshift parameter would be caused by a line-like structure around 4.5 keV only shown in the BI spectrum. However, the  $F$ -test resulted in a chance probability due to the statistical fluctuation of 16%, and hence we conclude it is not significant enough. We note that the spectra were also reproduced with an absorbed power-law model ( $\chi^2 = 47/33$  d.o.f.); the best-fit parameters were  $N_{\mathrm{H}} = (4.1^{+1.9}_{-1.8}) \times 10^{21} \text{ cm}^{-2}$  and  $\Gamma = 1.8 \pm 0.2$ . Consequently, owing to the limited photon statistics, such simple models were also marginally acceptable, but did not give a significantly improved fit.

## 4 Discussion

We found diffuse X-ray emission above 2 keV, for the first time, from the Suzaku and Chandra observations of 1RXS J170047.8–314442. The improvement of photon statistics with both satellites allows us to characterize quantitatively X-ray properties on this diffuse emission. Chandra revealed that there was no point source at the position listed in the RBSC. Moreover, at least within the ACIS-S3 field of view, no point sources were found to contribute to the diffuse X-ray emission. This diffuse emission had a circular shape with a spatial

extent of  $\sim 3'.5$ , much larger than the ROSAT PSF. In addition, the center position of the source was located  $\sim 1'$  away in the north direction from the RBSC position. The source extent ( $\sim 3'.5$ ) might cause the source characterization of 1RXS J170047.8–314442 to be somewhat inaccurate.

We discovered that the X-ray emission of 1RXS J170047.8–314442 was not axisymmetric and that the peak of the X-ray surface brightness was shifted by  $\sim 1'$  in the north-western direction from the center. The Suzaku XRTs did not enable us to resolve this spot-like excess emission; the possibility that a point source was superposed by chance in the line of sight to the diffuse source cannot be ruled out. The bright spot was located  $\sim 15''$  away from the Chandra ACIS-S3 field of view, and then no bright emission related to the spot was detected. Thus, the spot size was deduced to be  $\lesssim 30''$ . We searched the SIMBAD astronomical database<sup>2</sup> for other X-ray sources in the field of views of the Suzaku and Chandra observations. Only one unidentified X-ray source, 1RXS J170043.3–314131, was found. However, the source position is  $\sim 1'.4$  away from the bright spot in the north direction, as is shown in figure 1b. Assuming that excess X-ray emission was associated with the circular-shaped extended source, we modelled the non-axisymmetric surface brightness profile of 1RXS J170047.8–314442 with a  $\beta$ -model component of  $(\beta, r_c) = (1.02, 1'.51)$  plus a single point source.

The X-ray spectrum of 1RXS J170047.8–314442 was found to show an emission line at  $\sim 6$  keV. The XIS spectra were reproduced well (null hypothesis probability of 19%) with an absorbed thin thermal plasma model with  $N_{\mathrm{H}} = (2.4 \pm 0.4) \times 10^{21} \text{ cm}^{-2}$  and  $kT = 6.2 \pm 0.7$  keV. The averaged H I column density towards the source is  $1.8 \times 10^{21} \text{ cm}^{-2}$  (Dickey & Lockman 1990), significantly smaller than the fitted absorption column density. However,  $N_{\mathrm{H}}$  is still in a range of the spatial variation of the H I column density. Hence, the X-ray absorption is probably attributed to the Galactic interstellar medium.

<sup>2</sup> <http://simbad.u-strasbg.fr/simbad>

Assuming that the emission line was originated from highly ionized Fe ions (Fe XXV), the redshift parameter was determined to be  $z = 0.14$ .

The spatial morphology of the X-ray emission and the X-ray spectral properties strengthen that 1RXS J170047.8–314442 is indeed a cluster of galaxies, identified with CIZA J1700.8–3144. The X-ray determined redshift of  $z = 0.14 \pm 0.01$ , consistent with that of CIZA J1700.8–3144 ( $z = 0.134$ ), corresponds to the luminosity distance of 660 Mpc. The angular separation of  $1''$  is converted into 2.5 kpc. Therefore, the core radius of  $r_c = 1'.51$  is 220 kpc.

We estimated the total mass of the cluster, using the best-fit  $\beta$  model with  $(\beta, r_c) = (1.02, 1'.51)$ . Here the hydrostatic equilibrium and isothermality of the X-ray emitting gas were assumed. The total mass within a given radius is represented with

$$M(< r) = \frac{3\beta k T_e r^3}{G \mu m_H r_c^2} \frac{1}{1 + (r/r_c)^2}, \quad (1)$$

where  $k$ ,  $G$ ,  $\mu = 0.6$ , and  $m_H$  represent the Boltzmann constant, the gravitational constant, the mean molecular weight, and the mass of the hydrogen, respectively (Fabricant et al. 1980). The total mass within the whole source region was  $M(< 3'.5) = (3.1 \pm 0.9) \times 10^{14} M_\odot$ , where the error represents  $1\sigma$  confidence limit. We further calculated the overdensity radii of  $r_{500}$  and  $r_{200}$ , within which the averaged density is 500 and 200 times larger than the critical density of the universe ( $\rho_{\text{crit}} = 9.2 \times 10^{-30} \text{ g cm}^{-3}$ ).  $r_{500}$  and  $r_{200}$  were evaluated to be  $7.0r_c = 1.6 \text{ Mpc}$  and  $11r_c = 2.5 \text{ Mpc}$ , respectively.

To compare our result with scaling laws of clusters, e.g.,  $L_X$ – $T$  relation, in the literature, we evaluated the unabsorbed bolometric luminosity within  $r_{500}$ . The ARF was re-calculated for a circular region with a radius of  $r_{500} = 10'.6$  centered on  $(RA, Dec)_{J2000.0} = (17^{\text{h}}00^{\text{m}}48^{\text{s}}.8, -31^\circ 43' 49'')$ , the same as that of the whole source region. Using the new ARF, the unabsorbed bolometric flux and luminosity were deduced to be  $(1.1 \pm 0.1) \times 10^{-11} \text{ erg s}^{-1} \text{ cm}^{-2}$  and  $L_X(r < r_{500}) = (5.9 \pm 0.7) \times 10^{44} \text{ erg s}^{-1}$ , respectively. According to the  $L_X$ – $T$  relation derived from a cluster sample obtained with the Chandra observations (Maughan et al. 2012), this luminosity was by a factor of  $\sim 3$  lower than that expected from the X-ray emitting plasma with  $kT = 6.2 \text{ keV}$ . The authors pointed out that unrelaxed systems obeyed the  $L_X$ – $T$  relation with a steeper slope and a lower normalization than those of self-similar relaxed ones. The bolometric luminosity of  $L_X \sim 6 \times 10^{44} \text{ erg s}^{-1}$  was indeed consistent with that estimated from the  $L_X$ – $T$  relation of their unrelaxed cluster sample, by taking into consideration an intrinsic scatter of  $L_X$  for this subsample. Hence, CIZA J1700.8–3144 would be a cluster which is not dynamically relaxed yet.

Because of the limited photon statistics, we found no spatial variation of the plasma temperature at  $> 3\sigma$  confidence

level. Thus, in order to reveal the plasma dynamics, follow-up X-ray observations with longer exposures should be required. Because of the large collecting area and the good angular resolution of  $\sim 15''$ , XMM-Newton will be an appropriate observatory for the detailed spectroscopic study of CIZA J1700.8–3144. Furthermore, it should be necessary to conduct follow-up optical observations in more detail, in order to pick up more member galaxies. The spatial distribution and kinematics of the member galaxies may be available as a tracer of the dynamical process.

A deep radio observation will also be encouraged to unveil the dynamics of this cluster of galaxies. Radio halos or radio relics indicate the presence of high-energy electrons that may be originated from shock acceleration (e.g., Feretti et al. 2012). We note that there is an extended radio source, NVSS J170054–314338 (Condon et al. 1998), located near the center of CIZA J1700.8–3144 ( $\sim 1'.1$  away in the eastern direction, see cyan contours of figure 2). Nevertheless, the size of NVSS J170054–314338 is  $31''$  along the major axis and  $25''$  along the minor axis, much smaller than that of CIZA J1700.8–3144. Hence, the radio source may be neither radio halo nor radio relic associated with the cluster of galaxies.

## 5 Summary

We found that no point source was located at the position of 1RXS J170047.8–314442 with the Chandra observation. Instead, the Suzaku observation of 1RXS J170047.8–314442 revealed the presence of non-axisymmetric diffuse X-ray emission with a spatial extent of  $\sim 3'.5$ . The X-ray emission had a bright spot shifted by  $\sim 1'$  in the north-western direction from its center. Except for this bright spot-like emission, the surface brightness profile of 1RXS J170047.8–314442 can be explained with a single  $\beta$ -model with  $(\beta, r_c) = (1.02, 1'.51)$ .

The X-ray spectrum of 1RXS J170047.8–314442 was well reproduced with an absorbed optically-thin thermal plasma model; the absorption column density and the plasma temperature were determined to be  $(2.4 \pm 0.4) \times 10^{21} \text{ cm}^{-2}$  and  $6.2 \pm 0.7 \text{ keV}$ , respectively. Judging from the absorption column density, the X-ray source should be an extragalactic object. Assuming that the emission line at  $\sim 6 \text{ keV}$  is due to Fe XXV  $K\alpha$  emission, we estimated the X-ray redshift of  $z = 0.14 \pm 0.01$ .

The spatial morphology and spectral properties support that the origin of the X-ray emission is a hot gas associated with a cluster of galaxies, confirming the optical identification with CIZA J1700.8–3144 ( $z = 0.134$ ; Kocevski et al. 2007). The unabsorbed bolometric luminosity of  $L_X(r < r_{500}) = (5.9 \pm 0.7) \times 10^{44} \text{ erg s}^{-1}$ , which was consistent with that expected from the  $L_X$ – $T$  relation of the unrelaxed clusters (Maughan et al. 2012), indicates that CIZA J1700.8–3144 may be in an unrelaxed state.

## Acknowledgments

First of all, we are deeply grateful to Dr. Harald Ebeling for careful and fruitful comments to improve our manuscript. We would like to thank all the Suzaku team members for their support of the observation and useful information on the XIS and HXD analyses. The scientific results reported in this paper are also based on the observation made by the Chandra X-ray Observatory.

## References

- Anders, E., & Grevesse, N. 1989, *Geochim. Cosmochim. Acta*, 53, 197
- Balucinska-Church, M., & McCammon, D. 1992, *ApJ*, 400, 699
- Boldt, E. 1987, *Observational Cosmology*, 124, 611
- Burke, B. E., Gregory, J. A., Bautz, M. W., et al. 1997, *IEEE Transactions on Electron Devices*, 44, 1633
- Carollo, C. M., Ferguson, H. C., & Wyse, R. F. G. 1999, *The Formation of Galactic Bulges*,
- Cavaliere, A., & Fusco-Femiano, R. 1976, *A&A*, 49, 137
- Coldwell, G., Alonso, S., Duplancic, F., et al. 2014, *arXiv:1407.0262*
- Condon, J. J., Cotton, W. D., Greisen, E. W., et al. 1998, *AJ*, 115, 1693
- Dickey, J. M., & Lockman, F. J. 1990, *ARA&A*, 28, 215
- Fabricant, D., Lecar, M., & Gorenstein, P. 1980, *ApJ*, 241, 552
- Feretti, L., Giovannini, G., Govoni, F., & Murgia, M. 2012, *A&AR*, 20, 54
- Fruscione, A., et al. 2006, *Proc. SPIE*, 6270
- Ishisaki, Y., et al. 2007, *PASJ*, 59, 113
- Jonker, P. G., Bassa, C. G., Nelemans, G., et al. 2011, *ApJS*, 194, 18
- Kocevski, D. D., Ebeling, H., Mullis, C. R., & Tully, R. B. 2007, *ApJ*, 662, 224
- Kokubun, M., et al. 2007, *PASJ*, 59, 53
- Koyama, K., Makishima, K., Tanaka, Y., & Tsunemi, H. 1986, *PASJ*, 38, 121
- Koyama, K., et al. 2007, *PASJ*, 59, 23
- Maughan, B. J., Giles, P. A., Randall, S. W., Jones, C., & Forman, W. R. 2012, *MNRAS*, 421, 1583
- Mitsuda, K., Bautz, M., Inoue, H., et al. 2007, *PASJ*, 59, 1
- Mori, H., Maeda, Y., Ueda, Y., & Inoue, H. 2006, *The X-ray Universe 2005*, 604, 459
- Mori, H., Maeda, Y., Ueda, Y., Dotani, T., & Ishida, M. 2012, *PASJ*, 64, 112
- Mori, H., Maeda, Y., Furuzawa, A., Haba, Y., & Ueda, Y. 2013, *PASJ*, 65, 102
- Serlemitsos, P. J., et al. 2007, *PASJ*, 59, 9
- Takahashi, T., et al. 2007, *PASJ*, 59, 35
- Uchiyama, H., et al. 2009, *PASJ*, 61, 9
- Uchiyama, H., Nobukawa, M., Tsuru, T. G., & Koyama, K. 2013, *PASJ*, 65, 19
- Voges, W., Aschenbach, B., Boller, T., et al. 1999, *A&A*, 349, 389
- Weisskopf, M. C., Tananbaum, H. D., Van Speybroeck, L. P., & O'Dell, S. L. 2000, *Proc. SPIE*, 4012, 2